GDNF alleviates depression in Parkinson's disease by inhibiting α-synuclein aggregation and facilitating DA transmission from VTA to NAc

J Chen
Xuzhou Medical University
Z Ling
Xuzhou Medical University
MK Lv
Xuzhou Medical University
W Xu
Jinhu County People's Hospital
SZ Chen
Xuzhou Medical University
L Shao
Xuzhou Medical University
ZF Ma
Xuzhou Medical University
CX Wang
Xuzhou Medical University
YJ Song
Xuzhou Medical University
CX Tang
chxtang@xzhmu.edu.cn

Xuzhou Medical University

Research Article

Keywords: Parkinson's disease, alpha-synuclein, depression,; glial cell line-derived neurotrophic factor, dopamine D2-type receptors

Posted Date: November 12th, 2024

DOI: https://doi.org/10.21203/rs.3.rs-5365953/v1

Additional Declarations: No competing interests reported.

Abstract

Background Dopamine (DA) transmission from the ventral tegmental area (VTA) to the nucleus accumbens (NAc) is strongly implicated in the development of depression in Parkinson's disease (PD). We have observed a decrease in DA levels caused by alpha-synuclein (α-syn) aggregation, which has received limited attention regarding its association with depression in PD. This study investigated the role of VTA-related α-syn aggregation in depression of PD, and explored whether gial cell line-derived neurotrophic factor (GDNF) can inhibit α-syn aggregation thereby improving depressive symptoms.

Methods Here, α-syn aggregation and GDNF overexpression were induced in the VTA of C57BL/6J mice using adeno-associated viruses (AAV-SNCA, AAV-GDNF). Depression-like behavior was then evaluated, and the distribution of VTA- and NAc-related proteins, along with DA levels, were quantified. Subsequently, AAV-SNCA, AAV-GDNF, and cis-tracer virus were delivered into the VTA of DAT-cre mice via a cannula. The fluorescence intensity of the tracer in the VTA and NAc, as well as its colocalization with glutamate decarboxylase 67 isoforms (GAD67), were observed. Finally, in D2-cre mice, AAV-SNCA was injected into the VTA, and chemogenetic virus was infused into the ipsilateral NAc; depression-like behavior was then assessed before and after intraperitoneal administration of Clozapine N-oxide (CNO) in these mice.

Results The mice with increased phosphorylated-α-syn (p-α-syn) in the VTA exhibited depressiion-like behavior, along with decreased tyrosine hydroxylase (TH) in the VTA, reduced expression of synapse-associated proteins and dopamine D2-type receptor (D2R) in the NAc, and diminished levels of DA in both the VTA and NAc. However, GDNF overexpression in the VTA, led to a decrease in p-α-syn expression and reversed the aforementioned phenomena. Furthermore, results from cis-tracer virus and Immunofluorescence (IF) assay revealed a reduction in transmission of DA from the VTA to the NAc in mice with α-syn aggregation, which can be reversed by GDNF overexpression. Additionally, chemogenetic virus-induced activation of D2R in the NAc significantly ameliorated depression-like behavior due to α-syn aggregation in the VTA.

Conclusions The aggregation of α-syn within the VTA may play a crucial role in the pathogenesis of depression in PD, while GDNF can alleviate depression by inhibiting α-syn aggregation.

Background

Parkinson's disease (PD) is a common neurodegenerative disorder among middle-aged and elderly individuals[1]. The current consensus suggests that the main pathological hallmark of PD is the progressive degeneration and diminishment of dopaminergic neurons caused by α-synuclein (α-syn) aggregation in the midbrain, which results in dysfunction in the dopamine projection pathway, followed by typical motor dysfunction (e.g., bradykinesia, resting tremor, muscle rigidity and freezing of gait) as well as non-motor dysfunction (e.g., cognition, emotion, sleep and depression) [2]. Depression is a prevalent non-motor symptom in PD, and often precedes the onset of motor symptoms [3]. The presence of depression not only intensifies negative emotions, but also complicates patients’ lives and their

medication [4]. Although aberrant dopamine (DA) transmission has been implicated in the pathophysiology of various psychiatric disorders, including depression [5], the pathogenesis of depression in PD remains incompletely understood.

The midbrain limbic DA system plays a pivotal role in psychiatric disorders such as depression, with the main brain regions involved including the ventral tegmental area (VTA), nucleus accumbens (NAc), prefrontal cortex (PFC) and the Anterior Cingulate Cortex (ACC) [6]. Among these regions, the VTA is considered to be one of the major regions where DA neurons are predominantly located [7]. Light stimulation of the VTA-NAc pathway can modulate depression-like behaviors in animal models [8]. The efficacy of antidepressants in alleviating depressive symptoms is attributed to their ability to enhance the activity of DA neurons within the VTA and facilitate DA transmission along the VTA-NAc pathway [9-11]. Furthermore, the repeated deep brain stimulation (DBS) in the NAc led to an augmented activity of DA neurons in the VTA, potentially offering significant therapeutic advantages for individuals with exaggerated depression-like symptoms[12].

More than 95% of neurons in NAc are medium spiny neurons (MSN) expressing dopamine D1-type or D2-type receptors (D1R, D2R), and these neurons are output γ-aminobutyric acid (GABA) neurons [13, 14]. GABA is the main inhibitory neurotransmitter in mammalian central nervous system, which can directly play an antidepressant role through GABA type A receptors (GABAAR) [11]. In an animal model of depression induced by chronic unpredictable stress (CUS), a significant reduction was observed in both the DA levels and D2R expression within the NAc [15]. A study showed that NE-100, a sigma-1 receptor antagonist, reduced GABAAR, D2R in the NAc, causing depression-behaviors; conversely, quinpirole, a D2R agonist, injected into the NAc restored GABAAR levels and alleviated depressive behaviors in NE-100 mice [16]. D2R within the NAc may play a predominant role in depression of PD.

Clinical studies have demonstrated a positive correlation between the expression level of α-syn in the peripheral blood and the degree of depression [17]. α-syn is physiologically involved in the regulation of DA synthesis; and the overexpression of α-syn in DA neurons led to a reduction in both tyrosine hydroxylase (TH) activity and DA levels [18]. The aggregation of α-syn in PD may potentially impact DA transmission, thereby contributing to the development of depression. In addition, the findings of a study demonstrated that the antidepressant desipramine not only effectively alleviated depression-like behaviors in animal models of PD, but also exhibited a concurrent significant reduction in α-syn expression [19]. The targeting of α-syn aggregation may potentially offer a promising strategy to mitigate depression of PD.

The neurotrophic factor glial cell line-derived neurotrophic factor (GDNF) enhances the survival of DA neurons [20]. The serum GDNF level was significantly lower in clinical PD patients compared to the healthy population group [21]. A clinical retrospective study found that the GDNF level in peripheral blood was significantly lower in patients with major depression compared to the control group [22]. And an increase in GDNF level in the peripheral blood was observed after administering antidepressant drugs to patients with depression [23]. The addition of GDNF to primary cultured DA neuronal cells has been

demonstrated to effectively inhibit the aggregation of α-syn and consequently enhance neurons survival [24]. In view of the above, GDNF has the potential to alleviate the depression in PD by inhibiting the aggregation of α-Syn within the VTA.

The use of antidepressant medications, although partially effective in alleviating the symptoms, is accompanied by a fair share of side effects [25]. The potential of GDNF as a safer and more effective treatment for PD with depression renders it a promising option in addressing this dilemma.

Materials and methods

Animals

C57BL/6J male mice, D2-cre male mice and DA transporter (DAT)-cre male mice were used and housed in a facility with adjustable ambient temperature and humidity (23 ± 1.5°C, 45 ± 15%), with a 12h light-dark cycle (19:00 pm to 7:00 am). Experiments were performed using 8-12-week-old mice. All mice were acclimatized to this environment for a minimum of 7 days prior to the experiment. In the experiment, six or more mice were assigned to each group. The mice used in the experiments were obtained from Jiangsu Jicui Pharmaceutical and Chemical Biotechnology Co. as well as Saiye Model Biological Research Center Co. The use of these mice has been authorized under license No. SYXK [Su] 2018-0003 and 2018-0008.

Mouse brain stereotactic injection of adeno-associated virus (AAV)

Mice were deeply anesthetized with sodium pentobarbital (45 mg/kg) (merck, cat#57-33-0). Accorading to The Mouse Brain in Stereotaxic Coordinates (Second Edition), the anesthetized mice were immobilized on a stereotaxic apparatus for unilateral injections into the VTA (AP: -2.92 mm, ML: 0.45 mm, DV: -4.4 mm) or NAc (AP: 1.5 mm, ML: 0.75 mm, DV: -4.5 mm) using a trace syringe connected to a micro-injection pump. Mice were unilaterally injected with 0.3 μl of phosphate-buffered saline (PBS), AAV-SNCA (BrainVTA, cat#GT-0072), AAV-NC1 (BrainVTA, cat#PT-0142), AAV-GDNF (OBiO, Cat# Y12419), AAV-NC2 (OBiO, Cat# Y9957), or a mixed virus solution (in a ratio of 1: 1) individually. The micro-syringe was carefully inserted into the VTA or NAc, allowing for a stabilization period of 2 minutes. Then, solution was delivered at a rate of 0.06 μl per minute, allowing for a stabilization period of 5 minutes. Subsequently, the micro-syringe was gradually withdrawn, and the incision site on the scalp was sutured. After the surgical procedure, the mice were housed in a controlled warm environment and provided with peanuts as nutritional supplements. The behavioral experiments were performed after stable expression of the virus (approximately four weeks), followed by the perfusion and histology procedure.

The use of cis-tracer virus

Firstly, brain stereotaxic cannula was surgically implanted the VTA of DAT-cre mice at coordinates AP: -2.92 mm, ML: 0.45 mm, DV: -4.4 mm; subsequently, AAV-SNCA (α-syn mutant gene) and AAV-NC1

(negative control) were administered via the cannula. On the second day, PBS, AAV-GDNF, and AAV-NC2 were also administered via the cannula. On the third day, anterograde tracer (AAV-hSyn: BrainVTA, Cat# PT-1168) were also administered via the cannula. After a period of 4 weeks, the distribution of enhanced green fluorescent protein (EGFP) in the VTA and NAc were assessed using the Olympus BX43 microscope (Tokyo, Japan).

The use of chemogenetic virus

First, D2-cre mice were brain stereotaxic injection of AAV-SNCA in the VTA (AP: -2.92 mm, ML: 0.45 mm, DV: -4.4 mm), as well as cre-dependent chemogenetic virus AAV-hM3Dq (BrainVTA, cat# PT-0042), AAV-hM4Di (BrainVTA, cat# PT-0043) and control virus AAV-mCherry (BrainVTA, cat# PT-0013) in the NAc region (AP: 1.5 mm, ML: 0.75 mm, DV: -4.5 mm). After 4 weeks, mice in each group were injected with Clozapine N-oxide (CNO) (ApexBio, cat# A3317) or normal saline to directly activate or inhibit D2-MSN in NAc, and depression was evaluated by open field test, forced swimming test and tail suspension test within one hour.

In vitro cellular experimentation

MES23.5 DA cells (Otwo Biotech, Shenzhen, China) were cultured in dulbecco's modified eagle medium (DMEM) supplemented with 10% fetal bovine serum (FBS) and 1% penicillin-streptomycin (100 U/mL). The culture conditions comprised a controlled temperature of 37°C, a CO2 concentration of 5% and a humidity level set at 10%. Cells were passed twice per week. Sterile coverslips were previously arranged in a 24-well cell culture plate, and the cells were inoculated onto the coverslips. The 0.4 μM mutant form of α-syn pre-formed fibrils (PFF) (rPeptide, USA, Cat#S-1001) were initially administrated when the cells adhere to the surface and reach approximately 60%-70%. The Olympus BX51 microscope (Tokyo, Japan) and the Stereo Investigator v8.0 software (MicroBrightField Bioscience, VT, USA) were utilized for microphotography and cell counting. Cell counting was performed using a 10-fold objective lens and an unbiased counting frame.

Open field test (OFT)

Mice in Each group were subjected to OFT at postoperative week 4, and the degree of depression in mice was assessed by their distance traveled, number of grid crossing, and time spent in the center of the field. After setting up the experimental box, the ANY-maze software 7.33 (Stoelting Co., Wood Dale, IL, USA) was used to divide the site into 16 small squares, of which the middle 4 squares were the central area and the rest were the peripheral areas. After a 30-minute of acclimatization period, the labeled mice were placed sequentially into the center area of the field (disinfect the box with 75% alcohol after each test), while the video recording was started for 5 minutes.

Forced swimming test (FST)

Mice in Each group underwent FST at postoperative week 4, and the degree of depression in mice was assessed by the time spent floating in the water. The mice were acclimatized to the environment for 30

min before the experiment. The mice were subsequently placed in a plastic cylindrical tank (25 cm in height and 12 cm in diameter) filled with water (20 cm in height), while the water temperature was maintained at 23-25°C for a total of 6 minutes under dim-light conditions (white light). At the same time, time of immobility of the mice in the water was recorded and videotaped using ANY-maze software 7.33 (dry the mice after each test). Mice immobility is defined as that mice cease struggling only exerting effort to keep their heads above the water.

Tail-suspension test (TST)

Mice in each group were subjected to TST at postoperative week 4, the degree of depression in mice was assessed by the time the mice give up struggling to remain immobile. After a 30-minute of acclimatization period, the labeled mice were tied to the end of a wire horizontally positioned, 1 cm from the tail, so that the mice were suspended upside down on the wire with their heads approximately 15 cm above the ground. Each group of mice was separated by a white baffle. The mice were tail-suspended for 6 minutes, while recorded and videotaped using ANY-maze software.

Protein extraction program

After the mice were sacrificed, the entire brain was carefully stripped and placed on ice. The VTA and NAc regions were accurately excised unilaterally using a scalpel, with the fontanelle serving as a reference point. Protease inhibitor (KeyGEN, Cat# KGP610) was then added to the lysis buffer (Beyotime, Cat# P0013B) and the tissue was homogenized and then centrifuged (12,000 r/min, 20 min) at 4 °C to obtain the supernatant. Cellular protein extraction was performed in a similar manner. Following the removal of the culture medium, cells were washed twice with pre-cooled PBS. Subsequently, cell lysate (200 μL/dish) and protease inhibitor (2 μL/dish) were added. The lysed cells were gently scraped down using a cell spatula, and transferred into 1.5 mL centrifuge tubes with the aid of a pipette. All the centrifuge tubes were placed on ice and vortexed every 5 min, followed by centrifuged (14,000 r/min, 20 min) at 4°C to obtain the supernatant. Pipette the supernatant and transfer it to a new centrifuge tube, ensuring proper labeling, and store the protein at -80℃. Protein concentration in the supernatant was quantified by BCA Protein Assay (KeyGEN, Cat# KGP902). The optical density values were quantified using Multi-functional Microplate Tester (BioTek, Hercules, CA, USA).

Western blot (WB)

Equal quantities of protein from each group were separated by electrophoresis using sodium dodecyl sulfate polyacrylamide gel (SDS-PAGE), followed by transferred onto nitrocellulose membrane (BioTrace, Cat# P/N66485). The membranes were closed for 2 hours at room temperature (20-25°C) with 5% skimmed milk, which subsequently, were incubated overnight at 4°C with specified primary antibodies (α-syn, Abcam, Cat# ab138501; TH, Santa, Cat# sc-374048; p-α-syn, Thermo Fisher Scientific, Cat# PA5-37740; synaptosomal-associated protein 25 (SNAP-25), Santa, Cat# sc-20038; postsynaptic density protein 95 (PSD95), CST, Cat# 3450S; D2R, Santa, Cat# sc-5303; D1R, CST, Cat# #79777T; DAT, Santa, Cat# sc-32259; GDNF, Affinity, Cat# DF7727; glyceraldehyde-3-phosphate dehydrogenase

(GAPDH), huabio, Cat# ET1601-4; β-actin, Proteintech, Cat# 66009-l-lg). The membranes were washed three times with wash buffer, and then incubated with corresponding secondary antibodies (goat anti-rabbit IgG secondary antibody: Cat# 926-32211, goat anti-mouse IgG secondary antibody: Cat# 926-68070, LI-COR, USA) for 2 hours at room temperature. After three washes, protein expression on the membrane was detected using a dual infrared laser imaging system (Odyssey CLX, LI-COR, Inc., Lincoln, NE, USA), and analyzed using ImageJ software.

Freezing slices

Mice were anesthetized and subsequently perfused with pre-cooled normal saline to thoroughly remove all blood from the circulatory system. Following blood removal, the tissue was perfused with 4% paraformaldehyde for fixation. The brains were subsequently postfixed for 24 hours with 4% paraformaldehyde and then transferred to a 30% sucrose solution. Use a cryogenic slicing system (CM1950, Leica, Wetzlar, Germany) to cut the frozen brain into 20 μm coronal sections at -20°C. Brain sections were glued onto slides, dried at room temperature and stored in a slide box at -20℃.

Immunofluorescence (IF)

Cells were fixed in 4% paraformaldehyde for 20 minutes and then permeabilized with 10% phosphate buffered saline (PBS) containing 0.3% Triton-X-100 at room temperature. Cells were incubated overnight at 4°C with the corresponding primary antibodies (TH, Santa, Cat# sc-374048), which were subsequently blocked with 1% goat serum for 1 h. The next day, after three washes with 1% PBS, the cells were incubated with the appropriate secondary antibodies (Alexa Fluor 594，Abcam, Cat# ab150120) for 2 hours. Then they were washed more three times and stained with DAPI for 8 minutes. Similarly, brain tissue sections were washed three times with 0.1 M PBS, followed by blocking them with 0.2% Triton X-100 and 10% normal goat serum in 0.1 M PBS for 1 h. The sections were incubated overnight at 4°C with the corresponding primary antibodies (TH, Santa, Cat# sc-374048; p-α-syn, Millipore, Cat# MABN826; and glutamate decarboxylase 67 isoforms (GAD67), Abclonal, cat# A2938). The following day, after threes tims washes, the sections were incubated with secondary fluorescent antibodies (Alexa Fluor 488，Abcam, Cat# ab150077，Alexa Fluor 594，Abcam, Cat# ab150120) at room temperature. Then they were washed more three times and stained with 4',6-diamidino-2-phenylindole (DAPI) for 10 minutes. All image acquisition is performed using the Olympus BX43 microscope (Tokyo, Japan).

Enzyme-linked immunosorbent assay (ELISA)

The samples for the assay were pre-thawed at room temperature, and the standards were diluted to different concentrations with ddH2O in accordance with the instructions of the ELISA kit (DA ELISA Kit [mice]: Cat# NM-0355R2, MEIMIAN, Yancheng, Jiangsu, China). The standard wells were each added 50 μL of different concentrations of standards, while the blank wells and the sample wells were respectively prepared. The test sample (10 μL) and sample diluent (40 μL) were added to the designated wells, followed by the addition of enzyme reagent (100 μL) to each wel excluding blank wells. The mixtures were then incubated at 37℃ for 60 minutes. After washing, colorant A (50 μL) and colorant B (50 μL)

were added sequentially to each well for the reaction. The reaction was carried out at 37℃ for 15 minutes, and terminated by adding termination solution (50 μL). The optical density values of each well were measured using Multi-functional Microplate Tester (BioTek, Hercules, CA, USA).

Statistical analysis

The experimental data were analyzed using SPSS 22.0 (IBM SPSS Inc., Chicago, IL, USA), and the quantitative data were presented as mean ± standard errors. The data were assessed for the homogeneity of variance using Levene's test, as well as for normality using Shapiro-Wilk tests. If the data met the assumptions of the parametric test, comparisons between two groups utilized Student's t-test, whereas comparisons among multiple groups employed one-way analysis of variance (ANOVA) followed by Tukey's post-hoc test. The criterion for determining a statistically significant difference was set at $P < 0.05$. The statistical graphs were generated using GraphPad 8.0.2 and Adobe Illustrator 23.0.3 (Adobe, San Jose, CA, USA).

Results

The aggregation of α-synuclein leads to a decrease in DA levels within DA cells

The aggregation of α-syn in MES23.5 DA cells was induced using PFF as the initial step (Fig. 1A). Subsequently, the expression levels of α-syn and TH were assessed via WB after different durations of PFF exposure. The results from WB demonstrated a significant upregulation of α-syn expression and downregulation of TH expression in DA cells particularly in the 24h group compared to other groups (Fig. 1B-D). Furthermore, ELISA results also revealed that DA levels were significantly reduced in the 24h group compared to other groups (Fig. 1E). Additionally, IF analysis indicated a substantial decrease in the number of TH-positive cells following exposure to PFF for 24 hours when compared to the control group (Fig. 1F-G). These preliminary findings from our in vitro experiments suggest that α-syn aggregations can result in a decrease in TH expression and DA content in DA cell.

The aggregation of α-syn in VTA induces depression-like behavior in PD mice

The transmission of DA from the VTA to NAc is strongly associated with depression. Here, the involvement of α-synuclein aggregation in the pathogenesis of depression in PD was investigated, given its impact on dopamine levels. To achieve this, an adeno-associated virus of α-syn (AAV-SNCA) was stereotactically injected into the left VTA to establish PD mice model, followed by assessment of depression-like behavior in mice (Fig. 2A). The results of OFT demonstrated that mice in the AAV-SNCA group exhibited significantly reduced locomotor activity, as evidenced by decreased total distance traveled, fewer grid crossings, and decreased time spent in the central area compared to those in the AAV-NC group (Fig. 2B1-B4). The results of TST (Fig. 2C1, C2) and FST (Fig. 2C1, C3) revealed a significant augmentation in the duration of immobility observed within the AAV-SNCA group, as compared to the AAV-NC group. The IF results (Fig. 2D1, D2) demonstrated a significant increase in the distribution of p-α-syn within the VTA of the AAV-SNCA group compared to the AAV-NC group.

Conversely, a decrease in TH distribution within the VTA was observed in the AAV-SNCA group compared to the AAV-NC group (Fig. 2E1, E2). The WB results also demonstrated an increase in p-α-syn and a decrease in TH levels of AAV-SNCA group within the VTA, as compared to the AAV-NC group (Fig. 3B1-B3).

Weakened transmission of DA from VTA to NAc due to a-syn aggregation

Subsequently, the content of DA in the VTA and NAc was quantitatively determined by ELISA, thereby further evaluating the DA transmission from VTA to NAc. The results obtained from ELISA revealed a significant decrease in DA content within both regions of VTA and NAc in the AAV-SNCA group compared to the AAV-NC group (Fig. 3A). In the following, WB was performed to detect the relevant indicators in the NAc, showing a reduction in the expression of synapse-associated proteins (PSD95, SNAP-25) (Fig. 3C1-C3), DAT (Fig. 3C1, C3) and D2R (Fig. 3D1, D2) in the AAV-SNCA group compared to the AAV-NC group. However, there was no statistically significant difference observed in D1R expression between the AAV-SNCA group and the AAV-NC group (Fig. 3D1, D2). The implications of these findings suggest that the aggregation of α-syn within the VTA may serve as one of the underlying mechanisms contributing to the initiation of depression-like behavior via weaken activation of D2R.

GDNF inhibits α-syn aggregation and improves depression-like behavior in PD mice

To investigate whether GDNF can improve depression-like behavior in PD mice by inhibiting α-syn aggregation, an adeno-associated virus of GDNF (AAV-GDNF) was co-injected within the VTA in mice (Fig. 4A). The results of OFT demonstrated that mice in the AAV-SNCA + AAV-GDNF group exhibited significantly enhanced locomotor activity, as indicated by increased total distance traveled, more grid crossings, and an extended duration spent in the central area compared to those in the AAV-SNCA + AAV-NC group (Fig. 4B1-B4). The results of TST (Fig. 4C1, C2) and FST (Fig. 4C1, C3) demonstrated a significant reduction in immobility duration within the AAV-SNCA + AAV-GDNF group compared to the AAV-SNCA + AAV-NC group. Moreover, WB analysis showed a increased p-α-syn and a decreased TH within the VTA in the AAV-SNCA group compared to the Control group, which was subsequently reversed upon GDNF overexpression (Fig. 4D1, D2). Similarly, the reduction of SNAP-25, PSD95, DAT and D2R in the NAc induced by AAV-SNCA, was significantly reversed upon GDNF overexpression (Fig. D1, D3, D4); while the expression of D1R in the NAc does not exhibit any statistically significant differences among different groups (Fig. D1, D4). These findings implied the involvement of GDNF in DA transmission from VTA to NAc.

GDNF promotes DA transmission from VTA to NAc

To further substantiate the involvement of GDNF in dopamine transmission from the VTA to the NAc, DAT-cre mice were subjected to stereotactic embedding of cannulae in the VTA, and then sequentially injected with AAV-SNCA, AAV-GDNF, and cis-tracer virus (AAV-hSyn) (Fig. 5A). The IF results demonstrated a significant decrease in fluorescence intensity of DA neurons within the VTA and the NAc in the AAV-hSyn + AAV-SNCA + AAV-NC group compared to the AAV-hSyn + PBS + AAV-NC

group; however, an augment projection of DA neurons from the VTA to the NAc can be observed induced upon GDNF overexpression (Fig.5 B, C). Furthermore, the localization of GAD67 (a biomarker for MSN) and SYN (AAV-hSyn) in the NAc was achieved through IF staining. The area of GAD67 co-localized with SYN in the NAc was significantly reduced in the AAV-hSyn + AAV-SNCA + AAV-NC group, compared to the AAV-hSyn + PBS + AAV-NC group; however, the area of GAD67 co-localized with SYN in the NAc was significantly increased upon GDNF overexpression (Fig. 5D-G). GDNF overexpression within VTA reversed the attenuation of MSN activation due to α-syn aggregation, as evidenced by the WB results shown in Fig. 4D1-D4.

The activation of D2R in the NAc alleviates depression-like behaviour in PD mice

The results above pointed to the major involvement of D2R in depression. Thus, to investigate whether PD mice exhibit depression-like behavior due to abnormal activation of D2R in the NAc, a mouse model of PD was established using D2-cre mice via stereotaxic injections of AAV-SNCA into the VTA; subsequently, these mice were administrated with Cre-dependent chemical genetic virus into the NAc (Fig. 6A). The IF results demonstrated accurate viral injection of chemical genetic virus in the NAc (Fig. 6B). Next, behavioral tests were employed to assess the depression-like behaviour in mice.

The OFT results before and after intraperitoneal injection showed that the mice of the hM3Dq group exhibited significantly increased locomotor activity, frequency of grid crossings, and time spent in the central area after CNO injection, while those of the hM4Di group displayed a significant decrease in all measured parameters (Fig. 6C1-C3). Meanwhile, OFT results among different groups after intraperitoneal injection showed that mice in the hM3Dq + CNO group exhibited the best performance in terms of motor activity, frequency of crossing the grid, and time spent in the central region; on the contrary, these parameters were the least optimal in the hM4Di + CNO group (Fig. 6D1-D3).

Similarly, the TST and FST results before and after intraperitoneal injection showed that the immobility time of mice in the hM3Dq group was significantly shortened after CNO injection, whereas the immobility time of mice in the hM4Di group was increased (Fig. 6E1, E2). Additionally, the results of TST and FST after intraperitoneal injection revealed that mice in the hM3Dq + CNO group exhibited the shortest immobility time, while those in the hM4Di + CNO group displayed the longest immobility time (Fig. 6F). These findings suggested that D2R is major involved in the regulation of depression-like behaviour in PD mice.

Discussion

In this study, we reported that α-syn aggregation in PD leads to a reduction in DA transmission from VTA to NAc by downregulating DA levels, ultimately triggering depression-like behaviour due to attenuated D2-MSN activation. Importantly, our findings reveal that GDNF can effectively inhibit α-syn aggregation within the VTA and subsequently alleviate depression-like behaviors in PD mice.

Depression is one of the early non-motor symptoms in patients with PD, and clinical studies have shown a positive correlation between the the level of expression of the α-syn mutant gene SNCA in peripheral blood and severity of depression in PD patients [26, 27]. Under physiological conditions, α-syn is believed to play an important role in DA transmission, whereas under pathological conditions α-syn aggregates to form Lewy bodies and loses its normal function [28, 29]. Although, a large number of studies have demonstrated the association between α-syn and the development of mood disorders such as depression, the precise pathogenesis remains unclear [30]. The midbrain VTA is one of the major brain regions that produce DA and is involved in the regulation of mental and emotional changes in PD. In this study, we established a PD model by inducing α-syn aggregation in the VTA of mice. These PD mice exhibited depression-like behaviors, suggesting that SNCA overexpression in the VTA induces the α-syn aggregation and leads to the development of depression-like behaviors, which is consistent with the reported findings [31]. The aggregation of α-syn leads to internalization of N-methyl-D-aspartic acid receptor (NMDAR) subunit NR1 on the surface of DA neurons cultured in vitro, which is necessary for the assembly and function of NMDAR [32]. The impaired NMDAR function caused by α-syn aggregation may reduce the presynaptic calcium influx through the NMDAR and affects the calcium-independent regulation of calmodulin kinase [33], thereby reducing the synthesis of TH. The aforementioned studies provide robust support for our finding that our PD mice showed a significant aggregation of α-syn as well as a decrease in the expression of TH in the VTA. Similarly, reductions in TH expression and DA levels were observed after addition of pathologically aggregated α-syn to DA neurons in vitro.

The NAc, a brain region downstream of the VTA, contains over 95% of MSN, and its synaptic plasticity is involved in depression. Previous studies have shown that α-syn binds to vesicles located at neuronal synaptic terminals, thereby regulating the assembly of synapse-associated proteins [34]. Conversely, α-syn aggregation disrupts the assembly of synapse-associated proteins and impairs the transport of synaptic neurotransmitter vesicles [35]. In this study, the expression levels of synapse-associated proteins (e.g., SNAP-25, DAT and PSD95) in the NAc were significantly decreased after α-syn aggregation in the VTA, echoing the significant reduction of DA in both regions.

The role of DAT protein is to actively transport excessive DA from the synaptic gap back into the intracellular compartment, thereby ensuring the normal physiological function of synapses [36]. Erica et al. showed that 10-month-old transgenic mice expressing A53T mutation in α-syn exhibited decreased DAT expression and impaired DA uptake in the NAc as well as in the striatum [37], which is in agreement with the reduction of DAT protein in the NAc after α-syn aggregation in the VTA detected by the present study. α-syn may reduce DA uptake by decreasing DAT activity, leading to a further decrease in tissue DA levels. Our results from cis-tracer virus and IF assay showed diminshed transmission of DA from the VTA to the NAc in PD mice.

The role of DA is exerted via its receptors. The majority of MSN in the NAc express D1R and D2R, and numerous studies have shown that DA transmission plays an important role in depression [38, 39].Consistent with our results, α-syn aggregation in the VTA of PD model mice results in a decrease in DA levels and thus depression-like behaviors. Furthermore, there was a significantly reduction observed

in D2R expression within the NAc of PD mice, while no difference was detected in D1R. In the NAc, D1R and D2R play activating and inhibitory roles respectively, and the balance of the two is disrupted when DA-ergic fibers are depleted of their projections, leading to distinct alterations [40]. In the present study, we propose that a decrease in DA level in the NAc caused by α-syn aggregation in the VTA, results in attenuated activation of D2-MSN, followed by abnormal neurotransmitter release from the next level of interneurons, ultimately leading to depression-like behaviors. Therefore, we further validated the role of D2-MSN in NAc in regulating depression-like behaviors using D2-cre mice and chemogenetic viruses. The results showed that when D2-MSN was activated in the NAc of PD mice, depression-like behaviors improved; however, when D2-MSN was inhibited, depression-like behaviors worsened. It has been suggested in the literature that inhibition of D2R leads to a decrease in downstream phosphorylated protein kinase C expression, which in turn reduces GABA receptor expression and activation, thereby triggering mood disorders [41]. Thus, in the NAc, D2-MSN is mainly involved in regulating depression-like behaviors.

Currently, drugs used in the treatment of depression include 5-hydroxytryptamines, tricyclic antidepressants and DA reuptake inhibitors [42, 43]. However, the use of these drugs may exacerbate pre-existing movement disorders in PD patients or lead to other harmful side effects [25]. The studies have shown that GDNF has a protective effect on DA neurons [44], and lower levels of GDNF have been detected in the serum of PD patients compared to those of normal subjects [45]. Therefore, the present study investigated whether GDNF could improve the depression-like behavior caused by the pathological α-syn aggregation. The behavioral results showed that GDNF could improve the depression-like behaviors in PD mice, along with an increase in TH expression and a reduction in α-syn aggregation in the VTA. Consistent with previous findings, the addition of GDNF to in vitro cultured DA neurons inhibited further aggregation of exogenously α-syn pre-formed fibrils (PFF) [46]. In addition, the expression of synapse-associated proteins, such as SNAP-25 and PSD95, were increased, which could be attributed to GDNF inhibiting α-syn aggregation and thereby improving DA neurons survival. Moreover, the results from IF showed that overexpression of GDNF increased the number of co-labeling of DA synaptic endings in the NAc with the MSN marker GAD67; in other words, GDNF enhanced the activation of MSN in NAc by DA originating from VTA.

Conclusions

our work confirmed that GDNF can improve the depression-like behavior of PD mice by inhibiting α-syn aggregation in the VTA and promoting DA transmission from the VTA to the NAc (Fig. 7). The present study helps us understand the pathological role of α-syn in PD and provides a foundation for the clinical treatment of non-motor symptoms in PD. The pursuit of further investigations into specific mechanisms will be undertaken to enhance our understanding in this domain.

Abbreviations

AAV	Adeno-associated virus
ACC	Anterior cingulate cortex
α-syn	α-synuclein
CNO	Clozapine N-oxide
CUS	Chronic unpredictable stress
DA	Dopamine
DAPI	4',6-diamidino-2-phenylindole
DAT	Dopamine transporter
DBS	Deep brain stimulation
DMEM	Dulbecco's modified eagle medium
D1R	Dopamine D1-type receptors
D2R	Dopamine D2-type receptors
EGFP	Enhanced green fluorescent protein
ELISA	Enzyme-linked immunosorbent assay
FBS	Fetal bovine serum
FST	Forced swimming test
GABA	γ-aminobutyric acid
GABAAR	γ-aminobutyric acid type A receptor
GAD67	Glutamate decarboxylase 67 isoforms
GAPDH	Glyceraldehyde-3-phosphate dehydrogenase
GDNF	Glial cell line-derived neurotrophic factor
IF	Immunofluorescence
MSN	Medium spiny neurons
NAc	Nucleus accumbens
NC	Negative control
NMDAR	N-methyl-D-aspartic acid receptor
OFT	Open field test
PBS	phosphate buffered saline
PD	Parkinson's disease

PFC	Prefrontal cortex
PFF	Pre-formed fibrils
PSD95	Postsynaptic density protein 95
SDS-PAGE	Electrophoresis using sodium dodecyl sulfate polyacrylamide gel
SNAP-25	Synaptosomal-associated protein 25
TH	Tyrosine hydroxylase
TST	Tail-suspension test
VTA	Ventral tegmental area
WB	Western blot

Declarations

Ethics approval and consent to participate

Animal experimentation procedures were conducted in accordance with the guidelines for the Care and Use of Laboratory Animals developed by the National Institutes of Health and approved by the Institutional Animal Care and Use Committee of Xuzhou Medical University (approval number: 202209S042).

Consent for publication

All authors have approved the consent for publication of this manuscript.

Availability of data and materials

All data generated or analysed during this study are included in this published article.

Competing interests

The authors declare they have no competing interests

Funding

This work was supported by grants from the National Natural Science Foundation of China (82101263 to Tang CX), Postgraduate Research & Practice Innovation Program of Jiangsu Province (KYCX20_2444 to Chen J) and Innovation and Entrepreneurship Training Programme for University Students (202410313036Z).

Author Contributions

T.C. and C.J. conceived the project and designed the study; C.J. and L.Z. wrote the manuscript; C.J., L.Z., L.M., X.W., C.S., S.L., M.Z. and W.C. performed the experiments and acquired animal research data; S.Y. provided scientific input and English- editing work; C.J., S.Y. an T.C. contributed to analysis. All authors have read and agreed to the published version of the manuscript.

Acknowledgements

We would like to express our gratitude to all members of the Public Experimental Research Center and Experimental Animal Center of Xuzhou Medical University.

References

1. Hayes MT: **Parkinson's Disease and Parkinsonism**. *Am J Med* 2019, **132**(7):802-807.
2. Assogna F, Cravello L, Caltagirone C, Spalletta G: **Anhedonia in Parkinson's disease: a systematic review of the literature**. *Mov Disord* 2011, **26**(10):1825-1834.
3. Assogna F, Pellicano C, Savini C, Macchiusi L, Pellicano GR, Alborghetti M, Caltagirone C, Spalletta G, Pontieri FE: **Drug Choices and Advancements for Managing Depression in Parkinson's Disease**. *Curr Neuropharmacol* 2020, **18**(4):277-287.
4. Everitt BJ, Robbins TW: Neural systems of reinforcement for drug addiction: from actions to habits to compulsion. *Nat Neurosci* 2005, 8(11):1481-1489.
5. Hori H, Kunugi H: **Dopamine agonist-responsive depression**. *Psychogeriatrics* 2013, **13**(3):189-195.
6. Lobo MK, Nestler EJ: The striatal balancing act in drug addiction: distinct roles of direct and indirect pathway medium spiny neurons. *Front Neuroanat* 2011, 5:41.
7. Douma EH, de Kloet ER: Stress-induced plasticity and functioning of ventral tegmental dopamine neurons. *Neurosci Biobehav Rev* 2020, 108:48-77.
8. Jensen J, McIntosh AR, Crawley AP, Mikulis DJ, Remington G, Kapur S: **Direct activation of the ventral striatum in anticipation of aversive stimuli**. *Neuron* 2003, **40**(6):1251-1257.
9. Nieoullon A, Coquerel A: Dopamine: a key regulator to adapt action, emotion, motivation and cognition. *Curr Opin Neurol* 2003, 16 Suppl 2:S3-9.
10. Renard CE, Fiocco AJ, Clenet F, Hascoet M, Bourin M: Is dopamine implicated in the antidepressant-like effects of selective serotonin reuptake inhibitors in the mouse forced swimming test? *Psychopharmacology (Berl)* 2001, 159(1):42-50.
11. Pallis E, Thermos K, Spyraki C: Chronic desipramine treatment selectively potentiates somatostatin-induced dopamine release in the nucleus accumbens. *Eur J Neurosci* 2001, 14(4):763-767.
12. Song N, Liu ZH, Gao Y, Lu SS, Yang SL, Yuan C: NAc-DBS corrects depression-like behaviors in CUMS mouse model via disinhibition of DA neurons in the VTA. *Mol Psychiatr* 2024, 29(5):1550-1566.
13. Sesack SR, Grace AA: **Cortico-Basal Ganglia reward network: microcircuitry**. *Neuropsychopharmacology* 2010, **35**(1):27-47.

14. Meredith GE: The synaptic framework for chemical signaling in nucleus accumbens. *Ann N Y Acad Sci* 1999, 877:140-156.
15. Qiao H, Yang S, Xu C, Ma XM, An SC: Involvement of D2 receptor in the NAc in chronic unpredictable stress-induced depression-like behaviors. *Stress* 2020, 23(3):318-327.
16. Qin Y, Xu W, Li K, Luo Q, Chen X, Wang Y, Chen L, Sha S: Repeated inhibition of sigma-1 receptor suppresses GABAA receptor expression and long-term depression in the nucleus accumbens leading to depressive-like behaviors. *Frontiers in Molecular Neuroscience* 2022, 15.
17. Ishiguro M, Baba H, Maeshima H, Shimano T, Inoue M, Ichikawa T, Yasuda S, Shukuzawa H, Suzuki T, Arai H: **Increased Serum Levels of α-Synuclein in Patients With Major Depressive Disorder**. *The American Journal of Geriatric Psychiatry* 2019, **27**(3):280-286.
18. Lou H, Montoya SE, Alerte TNM, Wang J, Wu J, Peng X, Hong C-S, Friedrich EE, Mader SA, Pedersen CJ *et al*: Serine 129 Phosphorylation Reduces the Ability of α-Synuclein to Regulate Tyrosine Hydroxylase and Protein Phosphatase 2A in Vitro and in Vivo. *Journal of Biological Chemistry* 2010, 285(23):17648-17661.
19. Jeannotte AM, McCarthy JG, Sidhu A: Desipramine induced changes in the norepinephrine transporter, alpha- and gamma-synuclein in the hippocampus, amygdala and striatum. *Neurosci Lett* 2009, 467(2):86-89.
20. Zhu S, Li Y, Bennett S, Chen J, Weng IZ, Huang L, Xu H, Xu J: The role of glial cell line-derived neurotrophic factor family member artemin in neurological disorders and cancers. *Cell Prolif* 2020, 53(7):e12860.
21. Mamais A, Manzoni C, Nazish I, Arber C, Sonustun B, Wray S, Warner TT, Cookson MR, Lewis PA, Bandopadhyay R: **Analysis of macroautophagy related proteins in G2019S LRRK2 Parkinson's disease brains with Lewy body pathology**. *Brain Res* 2018, **1701**:75-84.
22. Yang Y, Xie B, Ju C, Jin H, Ye X, Yao L, Jia M, Sun Z, Yuan Y: The Association of Decreased Serum Gdnf Level with Hyperglycemia and Depression in Type 2 Diabetes Mellitus. *Endocr Pract* 2019, 25(9):951-965.
23. Martella G, Madeo G, Schirinzi T, Tassone A, Sciamanna G, Spadoni F, Stefani A, Shen J, Pisani A, Bonsi P: Altered profile and D2-dopamine receptor modulation of high voltage-activated calcium current in striatal medium spiny neurons from animal models of Parkinson's disease. *Neuroscience* 2011, 177:240-251.
24. Gu X, Mao X, Lussier MP, Hutchison MA, Zhou L, Hamra FK, Roche KW, Lu W: GSG1L suppresses AMPA receptor-mediated synaptic transmission and uniquely modulates AMPA receptor kinetics in hippocampal neurons. *Nat Commun* 2016, 7:10873.
25. Marwaha S, Palmer E, Suppes T, Cons E, Young AH, Upthegrove R: **Novel and emerging treatments for major depression**. *Lancet* 2023, **401**(10371):141-153.
26. Rossmann M, Sukumaran M, Penn AC, Veprintsev DB, Babu MM, Greger IH: Subunit-selective N-terminal domain associations organize the formation of AMPA receptor heteromers. *EMBO J* 2011, 30(5):959-971.

27. Zinsmaier AK, Dong Y, Huang YH: Cocaine-induced projection-specific and cell type-specific adaptations in the nucleus accumbens. *Mol Psychiatry* 2022, 27(1):669-686.
28. Gebara E, Zanoletti O, Ghosal S, Grosse J, Schneider BL, Knott G, Astori S, Sandi C: Mitofusin-2 in the Nucleus Accumbens Regulates Anxiety and Depression-like Behaviors Through Mitochondrial and Neuronal Actions. *Biol Psychiatry* 2021, 89(11):1033-1044.
29. Liu H, Jiang J, Zhao L: Protein arginine methyltransferase-1 deficiency restrains depression-like behavior of mice by inhibiting inflammation and oxidative stress via Nrf-2. *Biochem Biophys Res Commun* 2019, 518(3):430-437.
30. Brito V, Giralt A, Masana M, Royes A, Espina M, Sieiro E, Alberch J, Castane A, Girault JA, Gines S: Cyclin-Dependent Kinase 5 Dysfunction Contributes to Depressive-like Behaviors in Huntington's Disease by Altering the DARPP-32 Phosphorylation Status in the Nucleus Accumbens. *Biol Psychiatry* 2019, 86(3):196-207.
31. Yang M, Luo CH, Zhu YQ, Liu YC, An YJ, Iqbal J, Wang ZZ, Ma XM: 7, 8-Dihydroxy-4-methylcoumarin reverses depression model-induced depression-like behaviors and alteration of dendritic spines in the mood circuits. *Psychoneuroendocrinology* 2020, 119:104767.
32. Yu W, Yang W, Li X, Li X, Yu S: Alpha-synuclein oligomerization increases its effect on promoting NMDA receptor internalization. *Int J Clin Exp Pathol* 2019, 12(1):87-100.
33. Desce JM, Godeheu G, Galli T, Glowinski J, Cheramy A: Opposite presynaptic regulations by glutamate through NMDA receptors of dopamine synthesis and release in rat striatal synaptosomes. *Brain Res* 1994, 640(1-2):205-214.
34. Burre J, Sharma M, Tsetsenis T, Buchman V, Etherton MR, Sudhof TC: **Alpha-synuclein promotes SNARE-complex assembly in vivo and in vitro**. *Science* 2010, **329**(5999):1663-1667.
35. Wang L, Das U, Scott DA, Tang Y, McLean PJ, Roy S: **alpha-synuclein multimers cluster synaptic vesicles and attenuate recycling**. *Curr Biol* 2014, **24**(19):2319-2326.
36. Jayaramayya K, Iyer M, Venkatesan D, Balasubramanian V, Narayanasamy A, Subramaniam MD, Cho SG, Vellingiri B: **Unraveling correlative roles of dopamine transporter (DAT) and Parkin in Parkinson's disease (PD) - A road to discovery?** *Brain Res Bull* 2020, **157**:169-179.
37. Unger EL, Eve DJ, Perez XA, Reichenbach DK, Xu Y, Lee MK, Andrews AM: Locomotor hyperactivity and alterations in dopamine neurotransmission are associated with overexpression of A53T mutant human alpha-synuclein in mice. *Neurobiol Dis* 2006, 21(2):431-443.
38. Cabib S, Puglisi-Allegra S: **The mesoaccumbens dopamine in coping with stress**. *Neurosci Biobehav Rev* 2012, **36**(1):79-89.
39. Gershon AA, Vishne T, Grunhaus L: **Dopamine D2-like receptors and the antidepressant response**. *Biol Psychiatry* 2007, **61**(2):145-153.
40. Meurers BH, Dziewczapolski G, Shi T, Bittner A, Kamme F, Shults CW: Dopamine depletion induces distinct compensatory gene expression changes in DARPP-32 signal transduction cascades of striatonigral and striatopallidal neurons. *J Neurosci* 2009, 29(21):6828-6839.

41. Zhang T, Chen T, Chen P, Zhang B, Hong J, Chen L: MPTP-Induced Dopamine Depletion in Basolateral Amygdala via Decrease of D2R Activation Suppresses GABA(A) Receptors Expression and LTD Induction Leading to Anxiety-Like Behaviors. *Front Mol Neurosci* 2017, 10:247.
42. Ornoy A, Weinstein-Fudim L, Ergaz Z: Antidepressants, Antipsychotics, and Mood Stabilizers in Pregnancy: What Do We Know and How Should We Treat Pregnant Women with Depression. *Birth Defects Res* 2017, 109(12):933-956.
43. Hamon M, Blier P: **Monoamine neurocircuitry in depression and strategies for new treatments**. *Prog Neuropsychopharmacol Biol Psychiatry* 2013, **45**:54-63.
44. Zhu S, Zhao C, Wu Y, Yang Q, Shao A, Wang T, Wu J, Yin Y, Li Y, Hou J *et al*: **Identification of a Vav2-dependent mechanism for GDNF/Ret control of mesolimbic DAT trafficking**. *Nat Neurosci* 2015, **18**(8):1084-1093.
45. Chen G, Du Y, Li X, Kambey PA, Wang L, Xia Y, Tang C, Shi M, Zai-Li L, Zai EX *et al*: Lower GDNF Serum Level Is a Possible Risk Factor for Constipation in Patients With Parkinson Disease: A Case-Control Study. *Front Neurol* 2021, 12:777591.
46. Chmielarz P, Er S, Konovalova J, Bandres L, Hlushchuk I, Albert K, Panhelainen A, Luk K, Airavaara M, Domanskyi A: **GDNF/RET Signaling Pathway Activation Eliminates Lewy Body Pathology in Midbrain Dopamine Neurons**. *Mov Disord* 2020, **35**(12):2279-2289.

Figures

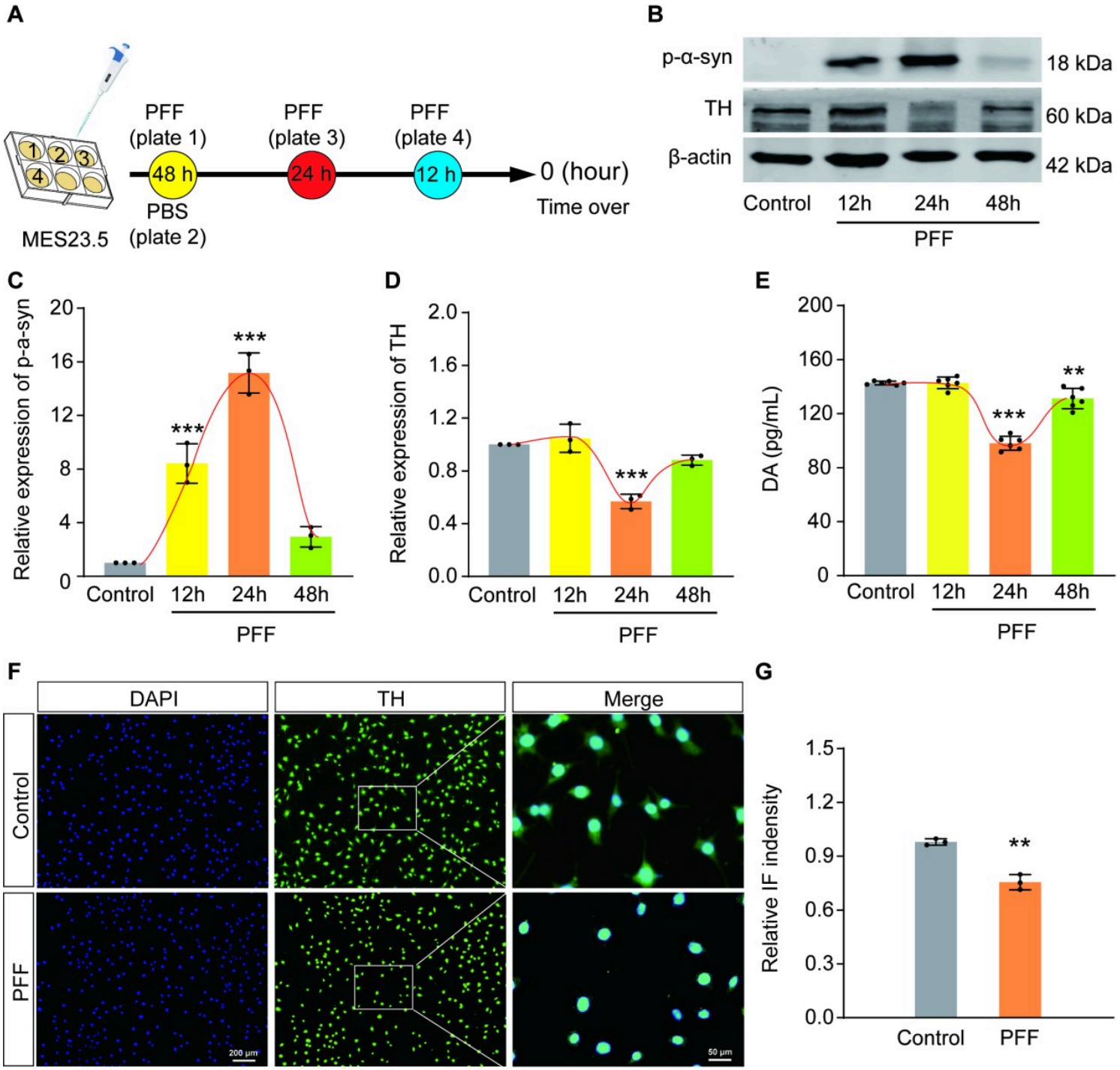

Figure 1

The administration of PFF led to a decrease in the expression of TH and the content of DA in MES23.5 dopamine cells

(A) The timeline of cellular experiments. (B-D) The WB results revealed that the MES23.5 dopamine cells of the PFF 24h group exhibited the highest level of p-α-syn expression and the lowest level of TH expression (n = 3, ***P < 0.001 vs. Control group). (E) ELISA results showed the lowest level of DA in 24h group (n = 6, ***P < 0.001, **P < 0.01 vs. Control group). (F, G) IF results showed that the decreased

distribution of TH+ positive cells in PFF group (scale bars: 200 μm, 50 μm) (n = 3, **P< 0.01 vs. Control group).

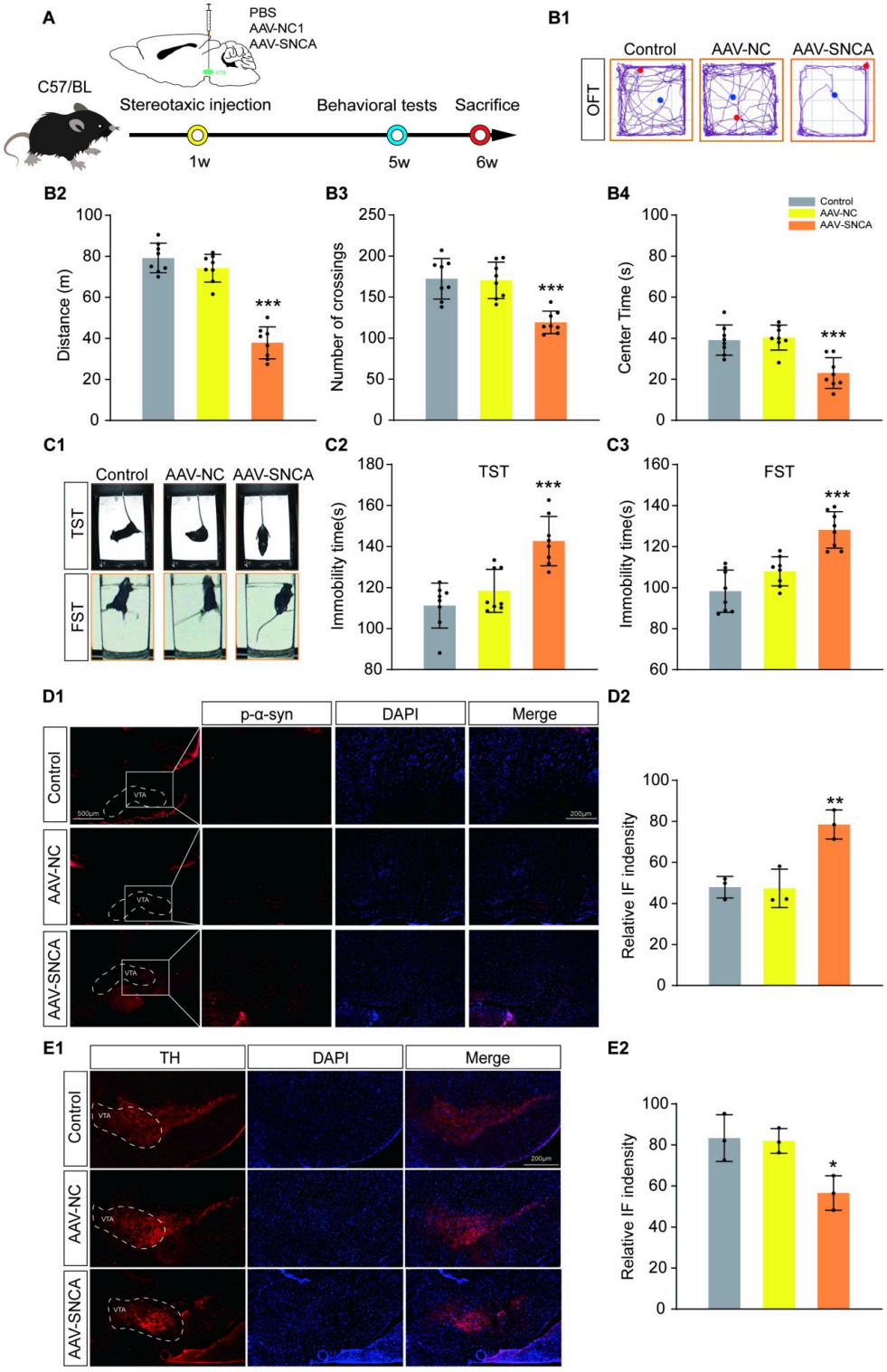

Figure 2

α-syn aggregation in the VTA induced depression-like behavior in PD mice.

(A) The timeline of mouse modeling and behavioral experiments. (B1-B4) The Representative traces of each group of mice in the open field experiment (blue point: starting position, red point: ending position and the statistical charts of the results of moving distance, grid crossings, and time spent in the central area (n = 8, ***P < 0.001 vs. AAV-NC group). (C1-C3) The results obtained from the TST and FST, showed a higher duration of immobility in mice of AAV-SNCA group compared to other groups (n = 8 per group ***P < 0.001 vs. AAV-NC group). (D1, D2) The IF results for the distribution of p-α-syn (red) in the VTA of mice in each group (scale bars: 200 μm, 200 μm) (n = 3, **P < 0.01 vs. AAV-NC group). (E1, E2) The IF findings regarding the distribution of TH (red) in the VTA of mice in each group. (scale bars: 200 μm, n = 3, *P < 0.05 vs. AAV-NC group).

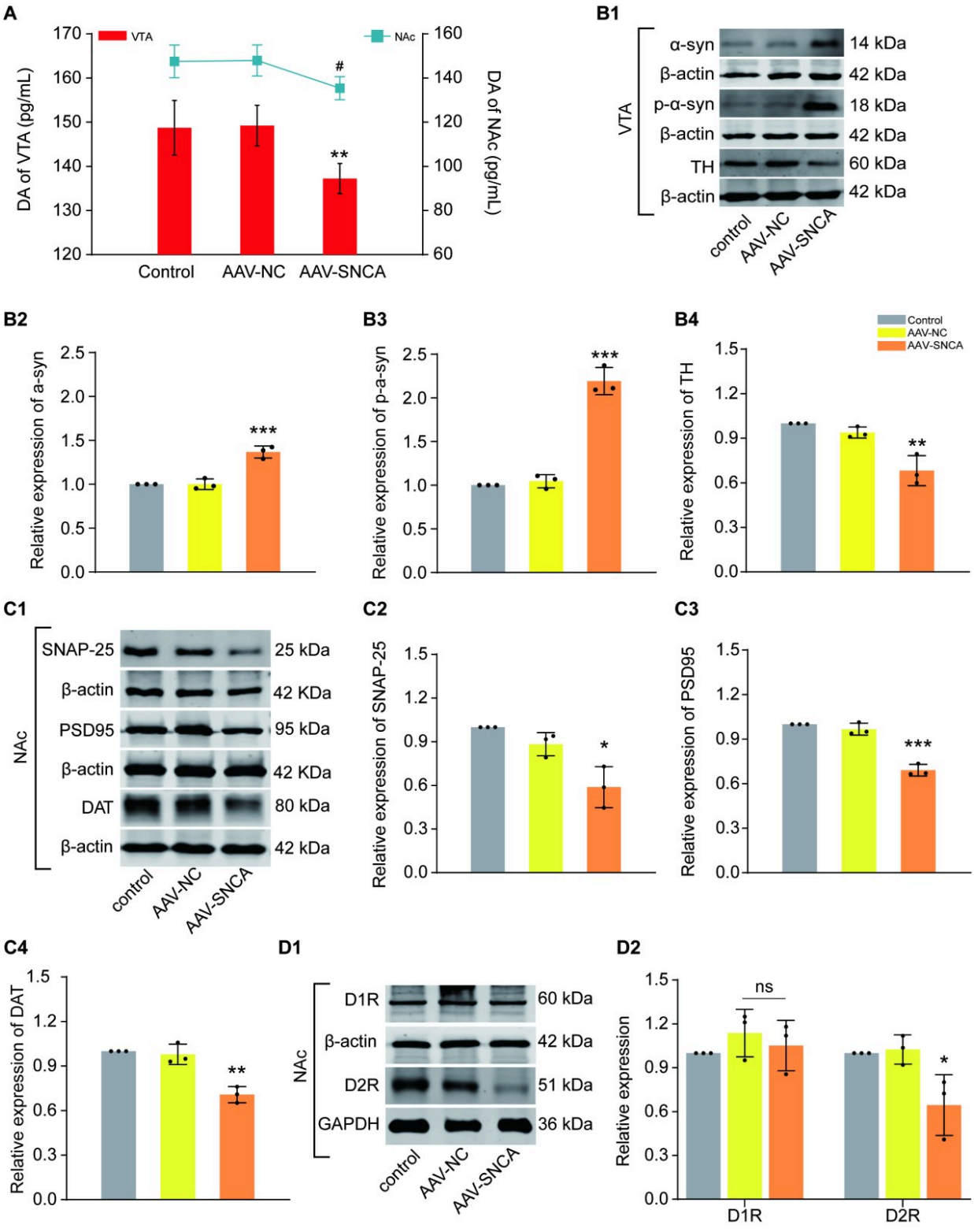

Figure 3

Weakened transmission of DA from VTA to NAc due to a-syn aggregation.

(A) ELISA was used to identify DA content in the VTA (left Y axis) and NAc (right Y axis) of mice in each group (n = 6, #$P < 0.05$, **$P < 0.01$ vs. AAV-NC group). (B1-B4) The WB results of α-syn, p-α-syn and TH in the VTA of mice in each group (n = 3, **$P < 0.01$, ***$P < 0.001$ vs. AAV-NC group). (C1-C4) The WB results

of SNAP-25, PSD95 and DAT in the NAc of mice in each group (n = 3, *P < 0.05, **P < 0.01, ***P < 0.001 vs. AAV-NC group). (D1, D2) The WB results of D1R and D2R in the NAc of mice in each group (n = 3, *P < 0.05 vs. AAV-NC group)

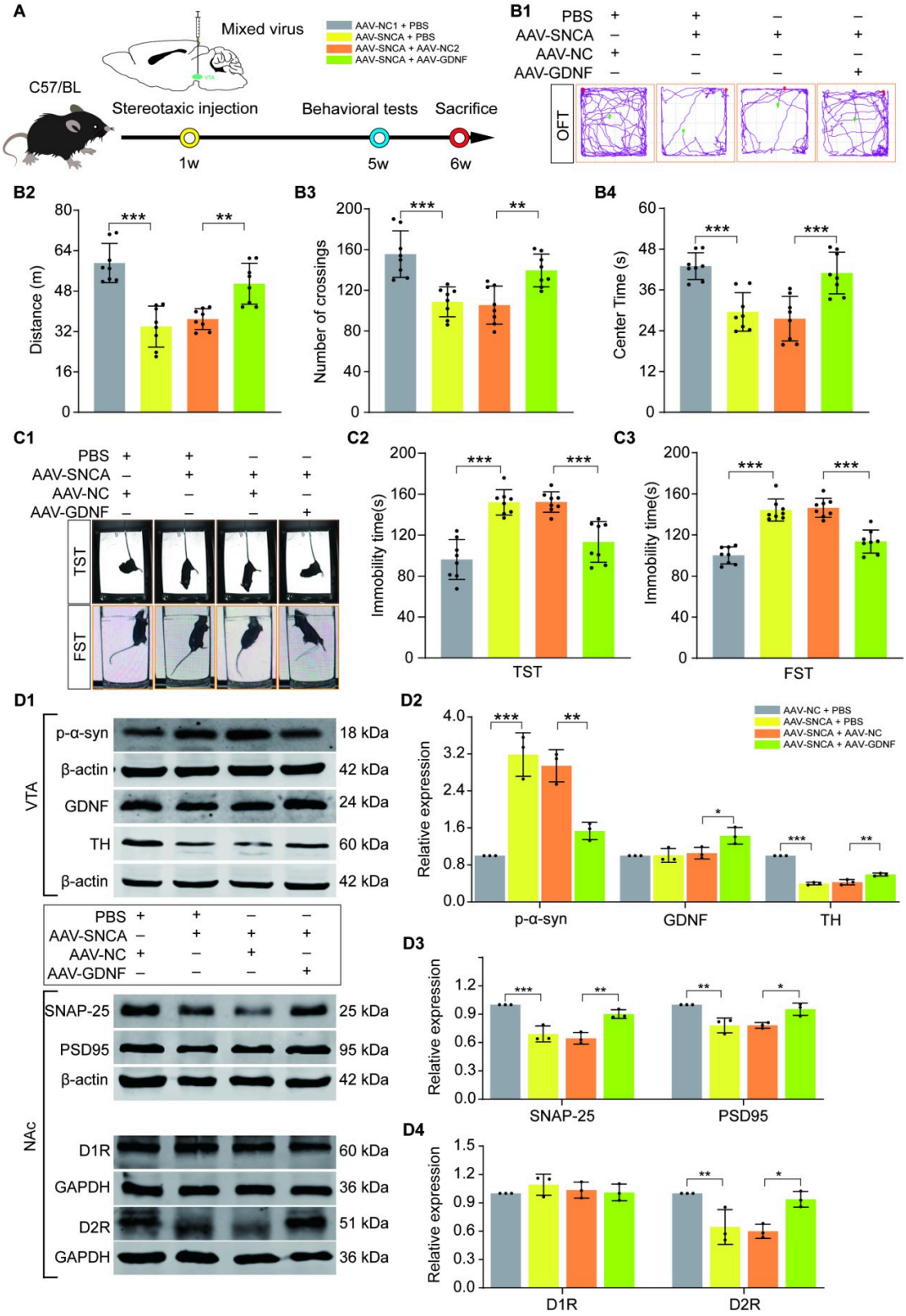

Figure 4

GDNF inhibited α-syn aggregation and improves depression-like behaviour in PD mice

(A) The timeline of mouse modeling and behavioral experiments. (B1-B4) The results of moving distance, grid crossings, and time spent in the central area of each group of mice in the OFT (green point: starting position, red point: ending position) (n = 8, $^{**}P < 0.01$, $^{***}P < 0.001$). (C1-C3) The results from TST and FST, showed the duration of immobility in mice of each group (n = 8, $^{***}P < 0.001$). (D1) The WB bands of p-α-syn, TH and GDNF in the VTA, as well as SNAP-25, PSD95, D1R and D2R in the NAc. (D2) The statistic diagram illustrating the expression levels of p-α-syn, TH and GDNF in the VTA (n = 3, $^{*}P < 0.05$, $^{**}P < 0.01$, $^{***}P < 0.001$). (D3) The statistic diagram illustrating the expression levels of SNAP-25 and PSD95 in the NAc (n = 3, $^{*}P < 0.05$, $^{**}P < 0.01$, $^{***}P < 0.001$). (D4) The statistic diagram illustrating the expression levels of D1R and D2R in the NAc (n = 3, $^{*}P < 0.05$, $^{**}P < 0.01$).

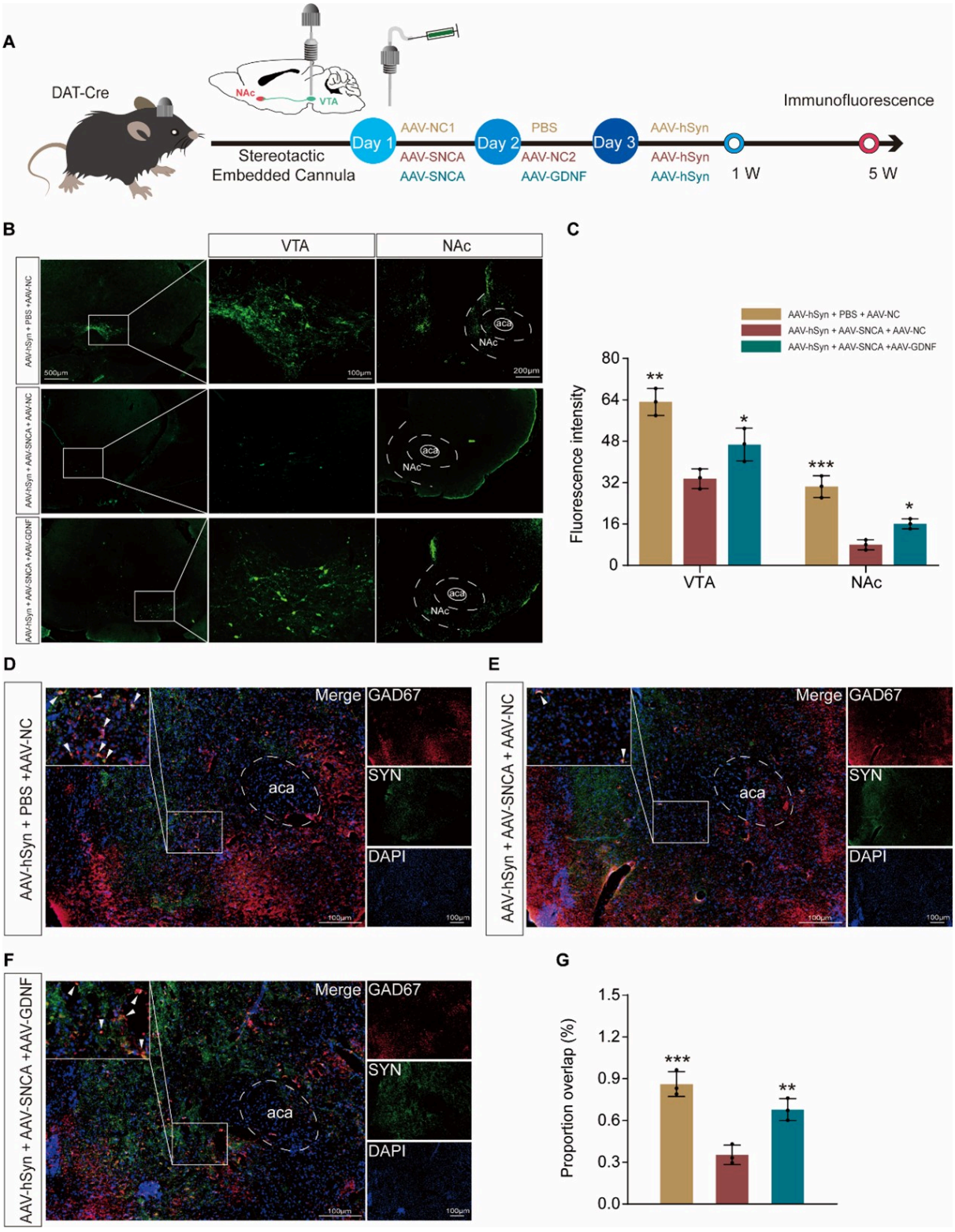

Figure 5

GDNF enhanced the transmission of DA from the VTA to the NAc.

(A) The schematic diagram of modeling and IF experiment timeline in each group of mice. (B-C) The IF staining was employed to examine the localization of the single anterograde tracer virus (labeled in green), aiming to detect the projection of DA neurons from the VTA to the NAc in each group of

mice(scale bars: 100 μm, 200 μm, 500 μm) (n = 3, *P< 0.05, **P < 0.01, ***P < 0.001 vs. AAV-hSyn + AAV-SNCA + AAV-NC group). (D-G) The IF staining showing the co-localization of DA synaptic terminals (labeled with SYN in red) and MSN (labeled with GAD67 in green) in the NAc of each group (scale bars: 100 μm, n = 3, **P < 0.01, ***P < 0.001 vs. AAV-hSyn + AAV-SNCA + AAV-NC group).

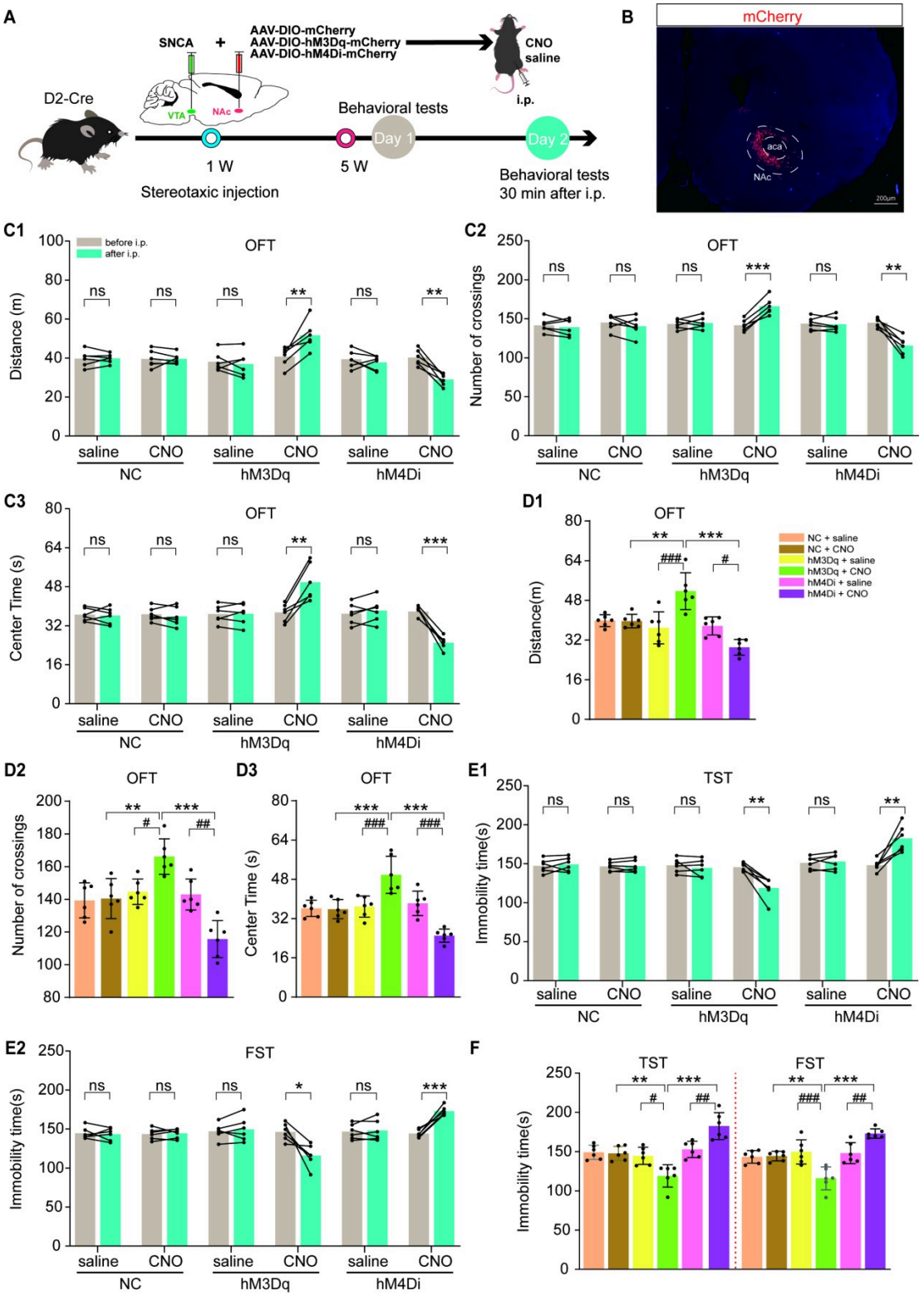

Figure 6

The activation of D2 receptor in the NAc can improve depression-like behavior in PD mice.

(A) The timeline of modeling and behavioral experiments in each group of mice. (B) The representative diagram illustrated the chemical genetic virus (red) in the NAc (scale bar: 200 μm). (C1-C3) The OFT results of self-comparison before and after intraperitoneal injection showed that only the mice of the hM3Dq and hM4Di groups exhibited statistically significant differences in movement distance, grid time, and dwell time in the central area after CNO injection (n = 6, $^{**}P < 0.01$, $^{***}P < 0.001$).(D1-D3) After intraperitoneal injection, the mice of the hM3Dq + CNO group exhibited the best performance in the OFT in terms of moving distance, grid times, and time spent in the central area; while, these parameters were the least optimal in the hM4Di + CNO group (n = 6, $^{**}P < 0.01$, $^{***}P < 0.001$, $^{\#}P < 0.05$, $^{\#\#\#}P < 0.001$). (E1, E2) The TST and FST results of self-comparison before and after intraperitoneal injection showed that only the mice of the hM3Dq and hM4Di groups exhibited statistically significant differences in immobility time after CNO injection (n = 6, $^{*}P < 0.05$, $^{**}P < 0.01$, $^{***}P < 0.001$). (F) After intraperitoneal injection, the mice of the hM3Dq + CNO group exhibited the shortest immobility time in both TST and FST; while, the mice of the hM4Di + CNO group exhibited the longest immobility time (n = 6, $^{**}P < 0.01$, $^{***}P < 0.001$, $^{\#}P < 0.05$, $^{\#\#}P < 0.01$, $^{\#\#\#}P < 0.001$).

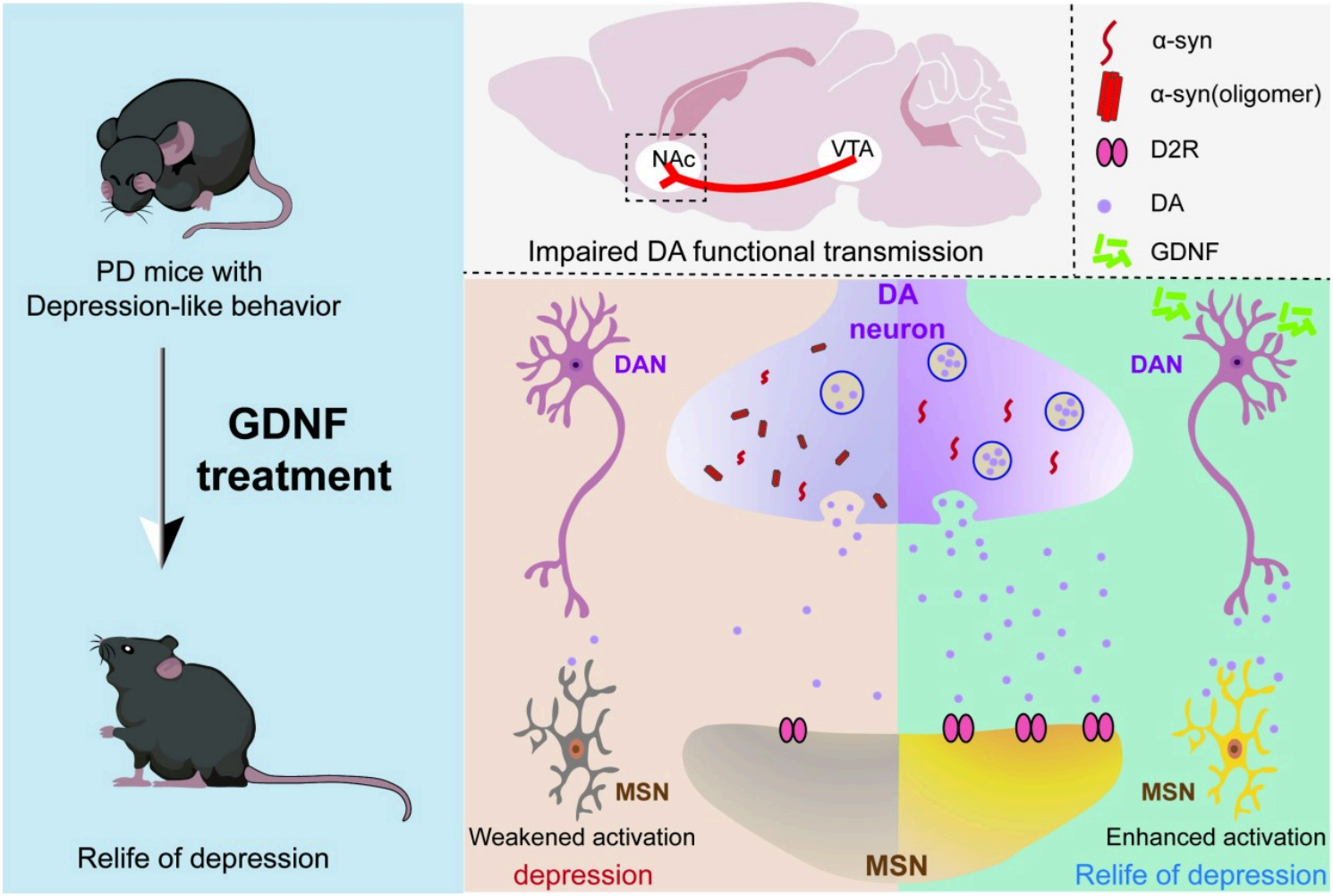

Figure 7

Summary diagram